Turkish Journal of Physics

Volume 27 | Number 3 Article 7

1-1-2003

Characterization of In_{4}Te_{3} Single crystals

M. DONGOL

M. M. NASSARY

M. K. GERGES

M. A. SEBAG

Follow this and additional works at: https://journals.tubitak.gov.tr/physics

Part of the Physics Commons

Recommended Citation

DONGOL, M.; NASSARY, M. M.; GERGES, M. K.; and SEBAG, M. A. (2003) "Characterization of In_{4}Te_{3} Single crystals," *Turkish Journal of Physics*: Vol. 27: No. 3, Article 7. Available at: https://journals.tubitak.gov.tr/physics/vol27/iss3/7

This Article is brought to you for free and open access by TÜBİTAK Academic Journals. It has been accepted for inclusion in Turkish Journal of Physics by an authorized editor of TÜBİTAK Academic Journals. For more information, please contact academic.publications@tubitak.gov.tr.

Turk J Phys
27 (2003) , 211 – 218.
© TÜBİTAK

Characterization of In_4Te_3 Single crystals

M. DONGOL, M. M. NASSARY*, M. K. GERGES, M. A. SEBAG
Physics Department, Faculty of Science, South Valley Uni, Qena-EGYPT
e-mail: Nassary_99@Yahoo.com

Received 29.11.2002

Abstract

Single crystals of In_4Te_3 grown by modified Bridgman technique were characterized by measurement of the Hall coefficient, electrical conductivity and Seebeck coefficient, in the temperature range 200-500 K. The investigated sample was found to be of P-type conductivity.R_H at room temperature was 3.1 $\times$ 10^{14}cm^3/coul and the carrier concentration was evaluated as 2.007 $\times$ 10^{14} cm^3. Energy gap ΔE_g and ionization energy ΔE_a were estimated as 0.28 eV and 0.12 eV, respectively, and the diffusion coefficient, the diffusion length, the mean free time between collision and the effective mass of carriers were evaluated. The variation of the Hall mobility with temperature was studied and hence the scattering mechanism is discussed.

Key Words: In_4Te_3, Hall and Seebeck coefficients, Electrical conductivity.

1. Introduction

Single crystal semiconductors have important practical applications in technology. For example, much better frequency stability and lower acoustic losses can be better achieved in single crystals than in polycrystalline aggregates. Great attention has been paid to the Ga-, In- and Tl- chalcogenides. In particular, the study of the $A_2^{III}B_3^{VI}-$, $A_2^{III}B_5^{VI}-$, and $A_4^{III}B_3^{VI}-$ compounds has been quite attractive.

Indium tellurides are useful as materials for electronics and for optical recording. Phase diagrams of In-Te systems can primarily attributed to the work of [1-7]. Compounds of $InTe_2$, In_9Te_7, In_4Te_3, InTe, In_3Te_4, α-In_2Te_3(low-temperature), β-In_2Te_3(high-temperature), In_3Te_5, In_4Te_7 and In_2Te_5 have been found to form in the In-Te system under standard conditions. The existence of the In_2Te, In_9Te_7, In_3Te_4 and In_4Te_7 phases are questionable [8]. The In_4Te_3 crystal structure has a Pearson symbol (oP28) and space group (Pnnm) [9]. J. H. C. Hogg et al. [10] summarise the unit cell parameters as, a = 1.5630 nm, b = 1.2756 nm, c = 0.4441 nm.

The present work is a study of some of the physical properties of the semiconducting telluride In_4Te_3 over the wide temperature range 200 –500 K in an attempt to obtain as much as possible information about the semiconducting properties of these compounds. The properties investigated were the electrical conductivity σ, Hall coefficient R_H and thermoelectric power α and then the dependence of these properties on temperature, where this is important for an investigation of transport phenomena in these materials. The work conducted is intended further the information about the electrical conduction, forbidden gap width and mobility of current carriers.

*Corresponding author

2. Experimental

2.1. Growth of single crystals and preparation samples

In_4Te_3 single crystal was synthesized by direct fusion method. This method is a new design [11] for crystal growth, based on the Bridgman technique and constructed in our laboratory. A silica ampoule was washed with both pure alcohol and doubly-distilled hot water. The ampoule was coated with a thin layer of carbon and then filled with spectroscopically standardized elements supplied by Aldirch with 99.999% purity. The correct proportion of the component materials was placed in the quartz ampoule. The silica ampoule was evacuated to 1.3×10^{-3} Pa before being sealed. The ampoule was moved through a three-zone tube furnace over a period fourteen days. In the first zone, the ampoule was held at a temperature above the melting point for about 24 hours. During the fusion process, the ampoule was frequently agitated to ensure homogeneity of the melt. With the aid of a mechanical system, the ampoule was then driven to the second zone. The zone temperature was held at about the melting point according to the phase diagram [8]. In the third zone the temperature was below the melting point, where crystallization proceeded until the ampoule solidified. The principles of the design and details of the process have been previously published in [11]. On removal from the furnace, the ingot appeared more gray-black, exihibiting reflection. The produced ingot was analyzed by X-ray analysis at the Central Metallurgical Research and Development Institute (CMRDI), Egypt. The results indicated that the ingot was good crystalline material with the required phase without any secondary phases. Conformation of the grown crystal showed that it had unit cell parameters as reported by J. H. C. Hogg et al. [10].

2.2. Characterization of the samples

For studying the electrical conductivity and Hall effect, the sample was prepared in a rectangular shape with dimension $7.5 \times 2.6 \times 1.3$ mm^3. Silver paste was used for the ohmic contacts. Measurement of the current-voltage characteristics showed that the contacts were ohmic. The conductivity and the Hall coefficient were measured by a compensation method in a special cryostat [12] with a conventional D.C. type potentiometer (type UJ 33E Mark) in a magnetic field of 5000 G which supplied from an Oxford N177 electromagnet. During the investigation, the temperature was varied 200-500 K. All measurements were carried out under vacuum at about 0.13 Pa.

For thermoelectric power (TEP) measurements, an evacuated calorimeter at 0.13 Pa was used to protect the sample from oxidation and water vapor condensation at high and low temperatures, respectively. The calorimeter was built with two heaters. The outer heater found the external source and discharged its heat slowly to the specimen environment. The inner heater was attached to the lower end of the crystal in order to control the temperature and its gradient along the specimen. The TEP is calculated at different temperatures by dividing the magnitude of the thermovoltage difference across the crystal by the temperature difference between the hot and cold ends.

3. Results and Discussion

3.1. Temperature dependence of electrical conductivity and Hall effect for In_4Te_3

Figure 1 shows the variation of electrical conductivity σ versus inverse temperature for In_4Te_3 single crystal. The relation shows quite clearly that, by increasing the temperature up the transition point (∼200K), the conductivity varies sharply with temperature. The rise of σ was interpreted as the increase in the number of charge carriers due to impurity ionization. At temperatures above the transition point, i.e. in the temperature range 280-400 K the conductivity remains almost temperature-independent. At high temperatures, 400-500 K, the conductivity increases sharply with increasing temperature, allowing us to measure the energy gap $\Delta E_g$from the slope of the curve, a value we calculate to be 0.28 eV. The room temperature conductivity has been found to be 107.9×10^4 ohm^{-1}.cm^{-1}. The Hall coefficient R_H was measured and found to have a positive variation with temperature, indicating that the holes are a major contribution to the conductivity. Figure 2 shows the temperature dependence of $R_H T^{3/2}$ as a fucuntion of inverse temperature and found to have behavior axpacted of semiconductors. The band-gap can measured

from this graph and found have a value of 0.24 eV. In the low temperature portion of the curve the ionization energy of the centers can be determined and was found to be 0.11 eV. The temperature dependence of the hole mobility of In_4Te_3 is shown in Figure 3. It was found that for temperatures $T > 200$ K the mobility decreases according as $\mu \sim T^{-2}$. This dependence indicates that the phonon scattering mechanism is responsible for the mobility in the high temperature range. The highest value of the hole mobility at 200 K is 362.96 cm^2/v.s. In addition, ionize impurities and other carriers may contribute to the scattering process within this range of temperature. Measurements of carrier density versus reciprocal temperature indicated that an acceptor level lies 0.12 eV above the valence band, as shown in Figure 4. In the temperature range 200-350 K, the carrier concentration in In_4Te_3 is determined by the number of ionize acceptors. Since the In_4Te_3 sample exhibits an intrinsic behavior above 400 K, the expected value for the intrinsic concentration can be given as [13]

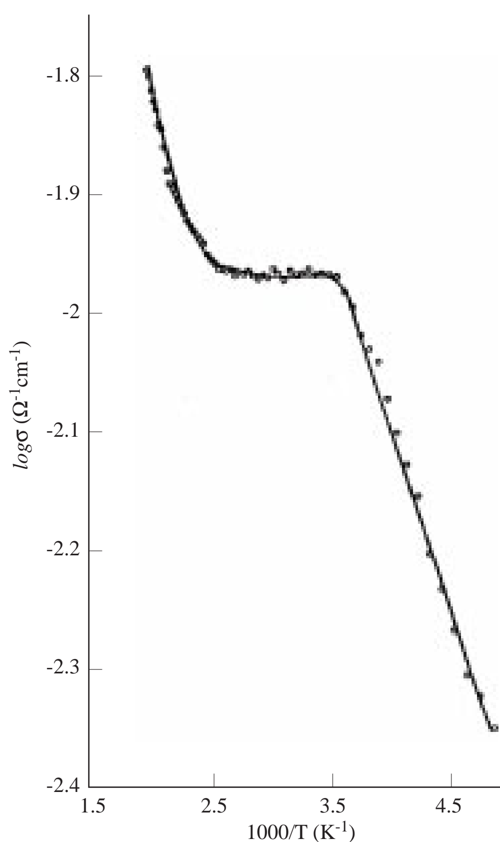

Figure 1. Temperature dependence of the electrical conductivity $ln_4 Te_3$.

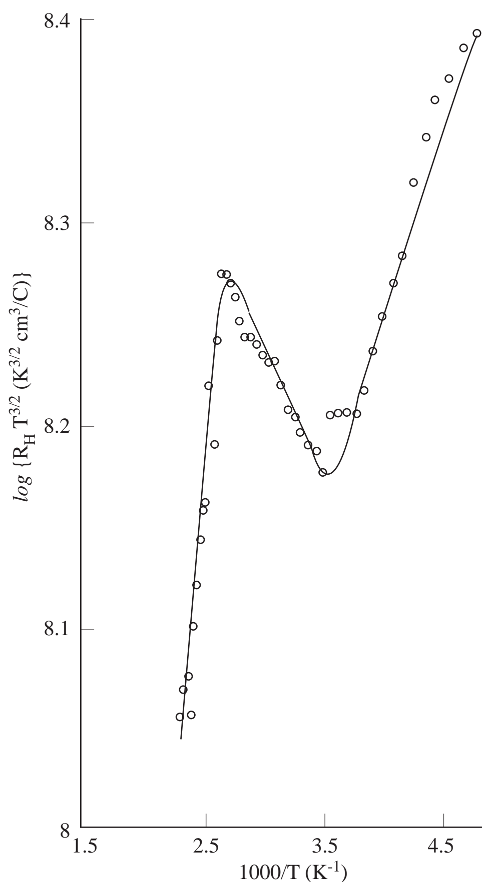

Figure 2. The relation between $R_H T^{3/2}$ and In_4Te_3.

$$n_i = 2(\frac{2\pi k}{h^2})^{3/2}(m_n^* m_p^*)^{3/4} T^{3/2} \exp(-\Delta E_g/2kT). \quad (1)$$

One can see that the carrier concentration varies sharply with increasing temperature. The value for the hole concentration at room temperature is 2.007×10^{14} cm^{-3}. The diffusion coefficient for holes is calculated to be 8.668 cm^2/s.

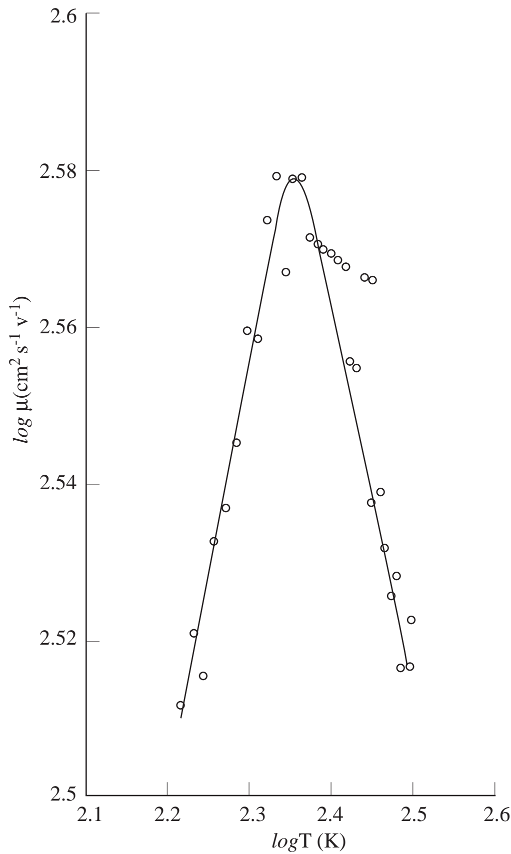

Figure 3. The behavior of Hall mobility as a function of temperature for In_4Te_3.

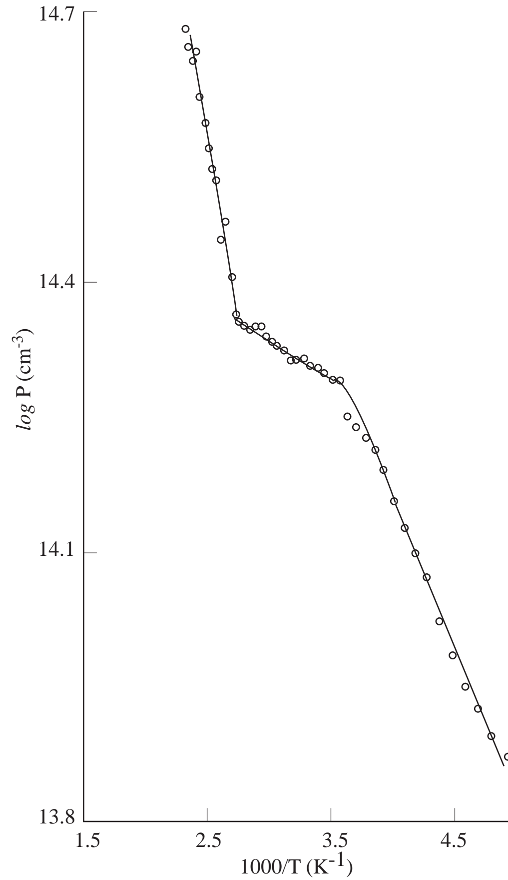

Figure 4. Variation of carrier concentration with temperature for In_4Te_3.

3.2. Temperature Dependence of the Thermoelectric Power for In_4Te_3

The temperature dependence of the thermoelectric power for In_4Te_3 is shown in Figure 5. Some features of these results may be pointed out as follows.

1. The thermoelectric power grows monotonically with temperature and shows a sharp maximum of $\alpha =$ 136 μV/K at T = 392 K. The rise of α is attributed to the thermal activation of the charge carriers in this range.

2. With a further rise in temperature a rapid fall in the thermoelectric power is noticeable. Such diminution of α, in this intrinsic range, is due to the fact that the direction of thermelectric fildes of the carriers is opposite to their energy flow and hence they attenuate each other.

3. The results show that In_4Te_3 samples have positive α over the entire temperature range, indicating a p-type conductivity of the investigated samples.

4. The room temperature of α value for In_4Te_3 amounted to 84 μV/K.

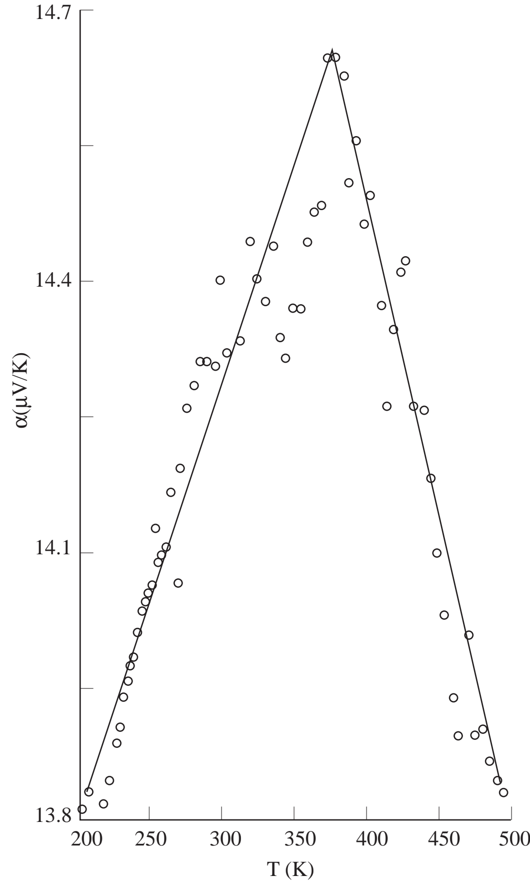

Figure 5. Temperature dependence of thermoelectric power of In_4Te_3.

The behavior of thermoelectric power with temperature in the intrinsic region can be described by the following equation [14]:

$$\alpha = -\frac{k}{e}\left[\frac{b-1}{b+1}\left(\frac{\Delta E_g}{2kT}+2\right)+\frac{1}{2}\ln\left(\frac{m_n^*}{m_p^*}\right)^{3/2}\right], \tag{2}$$

where b is the ratio of electron to hole mobility, ΔE_g is the energy gap and m_n^* , m_p^* are the effective mass of electrons and holes, respectively. This relationship is linear in inverse temperature. From the slope of the curve (in the intrinsic region) we calculated the ratio $b = \frac{\mu_n}{\mu_p} = 5$, using $\Delta E_g = 0.28$ eV. Thus using $\mu_p = 335.97\ \mathrm{cm}^2/$ vs at room temperature, then $\mu_n = 1679.85\ \mathrm{cm}^2/$ vs.

Figure 6. Shows a plot of α vs. $10^3/T$ for P-type In_4Te_3. The region negative slope indicates the increase of α with elevating surrounding temperature. Measurements of the temperature dependence of the electrical conductivity, the Hall coefficient and thermoelectric power enabled us to find the mean effective masses of the electrons and holes. Their ratio was evaluated from the intercept of the curve at $\frac{m_n^*}{m_p^*} = 1.3$ (we supposed here that $\frac{m_n^*}{m_p^*}$ dose not vary with temperature).

Wilson in 1953 suggested the following formula for use in the extrinsic region [15]:

$$\alpha = \frac{k}{e}\left[2 - \ln\frac{ph^3}{2(2\pi m_p^* kT)^{3/2}}\right] \tag{3}$$

Plotting Eq. (3) ln T against α, we obtain Figure 7. This appears that α decreases linearly with the increase of temperature in the temperature range corresponding to the extrinsic conductivity region, allowing the effective mass of the holes to be evaluated to $m_p^* = 4.6 \times 10^{-7} m_o$.

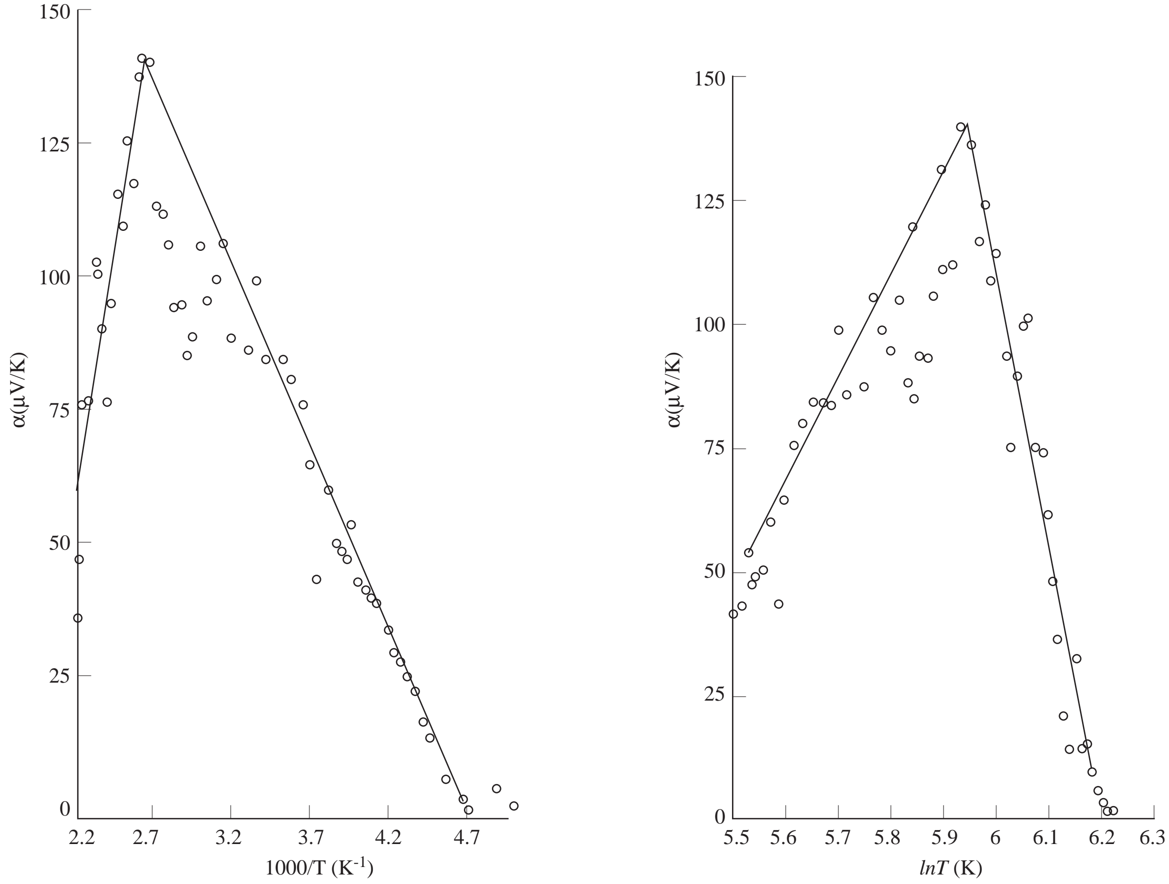

Figure 6. The relation between α and $10^3/T$ for In_4Te_3. **Figure 7.** The relation between α and ℓnT of In_4Te_3.

Combining this value with the above-mentioned results for, the ratio $\frac{m_n^*}{m_p^*} = 1.3$, we obtain $m_n^* = 3.5 \times 10^{-8}$ m_o for the effective mass of the minority carriers. Using the effective mass values of electrons and holes, the relaxation timeτ for both current carriers can be determined. For holes $\tau_p = 8.86 \times 10^{-16}$ s, whereas for electrons $\tau_n = 3.36 \times 10^{-16}$ s. The diffusion constants being related to the mobility of the charge carriers, we deduced as $D_p = 8.668$ cm^2/s and $D_n = 42.5$ cm^2/s, respectively. One can see that the diffusion constant inversely proportional to the effective mass of the holes and electrons. The electron mobility, as calculated, is much higher than the hole mobility; and this results is acceptable, since the hole effective mass is greater than that of the electron effective mass.

Another important parameter can be established, this being the diffusion length for holes and electrons. The value of L_p and L_n was found to be 8.7×10^{-8} cm and 11.95×10^{-8} cm, respectively. Figure 8. shows the dependence of thermoelectric power on the carrier density. We show that α increases sharply at beginning of the curve, and covers a temperature range 200-370 K and reaches a maximum value in the same transition region. After that, the value of thermoelectric power decreases exponentially with the carrier concentration. The general behavior of α as a function of P is quite similar to the temperature dependence of α. From this behavior we realize the effect of the charge carriers is a strong factor governing the variation of α. The same behavior was observed when we plotted α vs. $\ln \sigma$ for In_4Te_3 sample in Figure 9. This figure shows the dependence of thermoelectric power coefficient α on the natural logarithm of electrical conductivity according to [16]

$$\alpha = \frac{k}{e}\left[A + \ln\frac{2(2\pi m_p^* kT)^{3/2} 2e\mu}{(2\pi h)^3}\right] - \frac{k}{e}\ln\sigma. \tag{4}$$

The decrease of the thermoelectric power with electric conductivity may be due to the decreases of the carrier density in this range $T > 200$ K. Below 203 K it seems that TEP increases with the electric conductivity. The increase in the value of α in the low conductivity region may be due to the drag of carriers by phonons. From Figures 8 and 9, we can deduced that the variation of α with the environmental temperature is not a mobility effect, but is dependent on the variation of the concentration. The proposed treatment of the experimental data sheds new light on the main physical parameters in In_4Te_3 single crystal. The pronounced parameters obtained from TEP data gave evidence for practical applications.

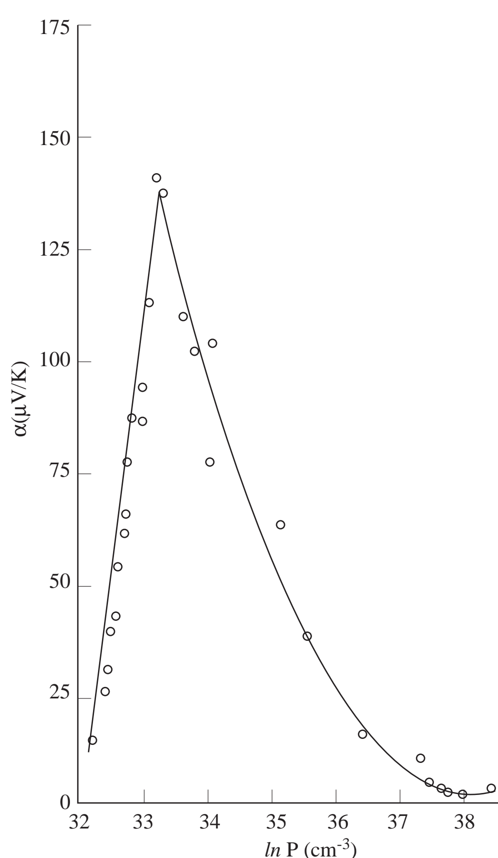

Figure 8. The relation between α and charge concentration of In_4Te_3.

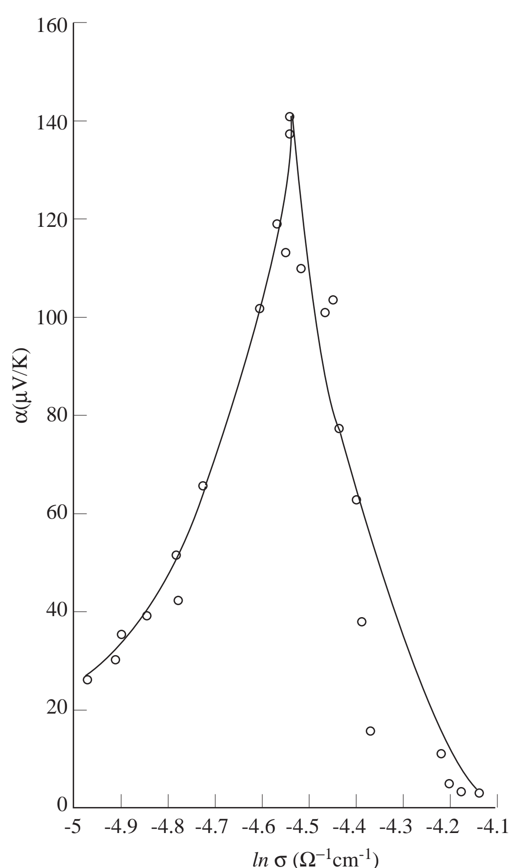

Figure 9. Variation of thermoelectric power with conductivity In_4Te_3.

4. Summary

We summarize out study of ln_4Te_3 single crystals as flows.

The temperature dependence of the electrical conductivity and Hall effect was investigated in the temperature range from 200 to 500 K for In_4Te_3 single crystal.

The positive values of both the Hall coefficient and thermoelectric power inticated that conductivity was p-type throughout the entire temperature range.

The crystal exhibited an energy gap of 0.28 eV and ionization energy of 0.12 eV.

References

[1] W. Klemm and H.U. Von Vogel, Z. Anorg. Chim., 219, (1934), 45–61(in German).

[2] E.G. Grochovski, D.K. Mason, G.A Schmidt, and P.H. Smith, J. Phys. Chem. Solids, 25, (1964), (6), 551.

[3] P.A. Shenk, Constitution of Binary Alloys, 2nd Suppl., McGraw-Hill Book Co., New York, NY, 1969.

[4] N.K. Abrikosov,V. F. Bankina,L. V. Porezkaya,E. N. Skudnova, and S. N. Chizhevskaya: Semiconducting Chalcogenides and Alloys Nauka, Moscwo, 1975 (in Russian).

[5] H. Okamoto and Charles E.T. White: Ser.Binary Alloy Phase Diagrams, 1991, vol. 338.

[6] C.S. Oh and D.N. Lee, CALPHAD, 1993, vol.17 (2), p. 175.

[7] Yves Feutelais and B. Legendre. Thermochim.Acta, 1998, vol. 314, pp. 37-53.

[8] V.P. Zlomanov, M.S. Sheiman, V.N. Demin and B. Legendre., J. phase Equilibria, vol. 22, no(3), (2001). PP, 339–344.

[9] H. Okamoto, P.R. Subramanian and Linda Kacprzak, Binary Alloy Phase Diagrams. ASM International (1990).

[10] J.H.C. Hogg, et al., ACTA CRYSTALLGRPHICA, SECTION B 1973, 29. pp. 2483.

[11] S.A. Hussein, and A.T. Nagat, to be published in Cryst. Research and Tech. March (1989).

[12] S.A. Hussein, *Cryst. Res. Technol.*, **24**, 6, 635 (1989).

[13] N. Cusack, the Electrical and Magentic Properties of Solids, c N. Cusack, New York (1958).

[14] J. Lauc, *J. Phys. Rev.,* **95** (1954) 1394.

[15] A.H. Wilson, Theory of Metals, 2nd ed., University Press, Cambridge 1953.

[16] P.H.E. Schmid and E. Mooser, *Helv. Phys. Acta.,* **45**, 870 (1972).